JOURNAL OF THERMOPHYSICS AND HEAT TRANSFER
Vol. 9, No. 3, July–September 1995

Ablation Analysis of the Shuttle Orbiter Oxidation Protected Reinforced Carbon–Carbon

S. D. Williams*
Lockheed Engineering and Sciences Company, Inc., Houston, Texas 77058
Donald M. Curry†
NASA Johnson Space Flight Center, Houston, Texas 77058
Dennis C. Chao‡
Rockwell International Corporation, Houston, Texas 77058
and
Vuong T. Pham§
NASA Johnson Space Flight Center, Houston, Texas 77058

Reusable, oxidation-protected reinforced carbon–carbon has been successfully flown on all Shuttle Orbiter flights. Thermal testing of the silicon carbide-coated, reinforced carbon–carbon to determine its oxidation characteristics has been performed in convective (plasma Arc-Jet) heating facilities. Surface sealant mass loss was characterized as a function of temperature and pressure. High-temperature testing was performed to develop coating recession correlations for predicting performance at the over-temperature flight conditions associated with abort trajectories. Methods for using these test data to establish multimission reuse (i.e., mission life) and single mission limits are presented.

Introduction

THE requirement for a reusable minimum weight thermal protection system (TPS) for the Space Shuttle Orbiter presented major material and design challenges. Ceramic materials were selected for most areas of the Orbiter external surface, but reinforced carbon–carbon (RCC) was selected for high-temperature regions where reusable surface insulation (RSI) could not safely be used as TPS. RCC has been successfully reused in these high-temperature regions on the Shuttle Orbiters, since the first flight of the Columbia vehicle (April 1981).

Oxidation protection of the RCC material is accomplished in a three-step process. Initial protection is provided by converting the outer carbon surface to silicon carbide (SiC) in a diffusion coating process. Secondly, further oxidation resistance is obtained by impregnation with tetraethyl–orthosilicate (TEOS). When cured, TEOS leaves a silicon dioxide (SiO_2) residue throughout the coating and carbon substrate. The third step is the application of a surface sealant (type A, sodium silicate/SiC mixture) to fill any porosity or microcracks on the surface. Even with this oxidation protection system, the RCC material still loses mass over an extended temperature range without any apparent surface recession.

Presented as Paper 94-2084 at the AIAA/ASME 6th Joint Thermophysics and Heat Transfer Conference, Colorado Springs, CO, June 20–23, 1994; received Aug. 8, 1994; revision received Dec. 28, 1994; accepted for publication Jan. 9, 1995.

*Consultant. Senior Member AIAA.
†LESS Subsystem Manager, Structures and Mechanics Division. Member AIAA.
‡Technical Specialist, Space Systems Division, Payloads Systems Engineering. Member AIAA.
§Senior Engineer, Structures and Mechanics Division. Member AIAA.

The most important parameter in the determination of RCC mission life is the oxidation of the carbon substrate that occurs as a result of oxygen penetrating the protective coating. The resultant strength degradation caused by substrate mass loss restricts the mission life capability since the RCC will be unable to sustain the imposed flight loads. Medford[1,2] developed analytical methods for predicting subsurface RCC oxidation performance including chemical kinetics at the subsurface oxidation sites, diffusion of oxygen into the coating fissures, growth of product film on the coating external surface and fissure walls, and differential thermal expansion between coating and substrate. These initial analyses used the experimental data of McGinnis[3] for a RCC material without TEOS and surface sealant. Subsurface mass loss testing for RCC impregnated with TEOS and the type A surface sealant was conducted in 1984[4,5] and 1990[6] to develop mass loss correlations (radiant and convective) for predicting the mission life of Orbiters Columbia, Atlantis, and Discovery.

The RCC was originally developed to have nominal multimission capability with a maximum temperature of 1811 K (2800°F). However, the extended operational flight envelope of the Orbiter and abort conditions can result in RCC surface temperatures significantly higher than the original design value. Requirements to increase the Orbiter range capability during certain abort conditions result in predicted RCC surface temperatures in excess of 2088 K (3300°F), causing RCC surface recession. To quantify RCC performance over the range of temperatures and pressures for these abort conditions, an over-temperature test program[6] was conducted. This data was used by Curry[7] to establish a single mission limit RCC temperature. Thus, there has been an ongoing effort to characterize the oxidation performance of the RCC surface coating material at these higher temperatures.

A second application of the sodium silicate sealant [i.e., double type A (DTA)] was made to the RCC components installed on the Orbiter Endeavor in order to increase mission life by decreasing the subsurface oxidation. Subsequently, the test program has been expanded to characterize the oxidation performance of the RCC with the DTA sealant.

Past efforts to characterize SiO_2/SiC/C systems have generally been conducted in a laboratory environment. This in-

vestigation differs from these efforts by analyzing the oxidation of the complex RCC material system in a high temperature Arc-Jet air environment simulating flight entry conditions.

This article utilizes data from the Johnson Space Center (JSC) over-temperature and DTA convective mass loss test programs to develop an analytical method for predicting the RCC sealant/coating (sodium silicate/silicon carbide) erosion and substrate oxidation. A nonequilibrium, chemically reacting boundary-layer program is used to predict Arc-Jet test and flight heating conditions. Utilizing the ablation model, correlated with Arc-Jet test data, mass loss predictions/mission life of the RCC oxidation protection coating are presented for typical flight entry conditions.

RCC Oxidation Tests

Successful RCC flight experience and an expanded operational flight envelope have led to higher heating rates and temperatures. An over-temperature test program has been conducted at these higher heating conditions to quantify RCC performance. This test program has provided the database to develop surface mass loss correlations.

DTA was applied to the RCC components installed on the Orbiter Endeavor as part of the baseline carbon system to further decrease subsurface mass loss and increase mission life. Orbiters Columbia, Atlantis, and Discovery also have selected RCC components with DTA sealant as a result of replacement activity. Accordingly, the test program was expanded to characterize the increased oxidation protection of the RCC with the DTA sealant.

Test Specimen and Procedures

All test and calibration specimens were 7.1-cm- (2.8-in.-) diam 19-ply discs of RCC (Fig. 1). The calibration specimens have three type C (tungsten, 5% rhenium/tungsten, 26% rhenium) thermocouples installed as shown in Fig. 1. TC #1 and TC #3 sense front surface temperatures, and TC #2 senses the back surface temperature.

Forty DTA specimens and four calibration models were available for testing. The specimens were fabricated from AVTEX RCC substrate:

Coated/TEOS/DTA specimen: silicon carbide coated, impregnated with TEOS and sealed with DTA surface sealant enhancement.

Sixty-two test specimens and seventeen calibration models (instrumented with thermocouples) were available in the over-temperature test program. There were three classes of specimens that were fabricated from either AVTEX or ENKA RCC substrate:

Coated/TEOS/type A specimen: silicon-carbide-coated, impregnated with TEOS and sealed with type A surface enhancement,

Coated/TEOS/no type A specimen: silicon-carbide-coated, impregnated with TEOS, but not sealed with type A surface enhancement,

Uncoated/TEOS specimen: RCC substrate, impregnated with TEOS.

Test specimens were photographed, weighed, and thickness measurements made prior to and after testing. Specimens were handled with clean white gloves and weighed to within 0.1 mg. Aluminum bags were used to prevent absorption of atmospheric moisture while the specimens were being weighed. Prior to weighing, the specimens were placed inside aluminum bags that were then placed inside a 149°C (300°F) oven for 4 h to remove water of hydration. The aluminum bags were then sealed, and the specimens allowed to cool prior to weighing. After the specimens had been tested, the specimens were cooled under vacuum in the test chamber for 25 min to minimize oxidation of the carbon substrate during repressurization.

Although the calibration models were instrumented with three type C thermocouples, an optical pyrometer operating at 0.865 μm was also used as a secondary, nonintrusive surface temperature measuring device. During the calibration runs, the pyrometer matched the readings from the surface thermocouples with an emissivity correction factor to account for the window and the mirror loss of 0.68 as in previous RCC test programs.[6] The desired surface pressures in the test matrix were measured with a 10.03 cm o.d. water-cooled pressure model. The pressure model and the test specimen with holder have the same outside diameters.

The test program was performed in both test chambers of the NASA/JSC Atmospheric Re-entry Materials and Structures Evaluation Facility (ARMSEF).[8] Test gases (23% O_2 and 77% N_2 by mass) are heated by a segmented, constricted arc heater and injected in a vacuum chamber through a water-cooled conical nozzle that has a 15-deg half-angle. During testing, the chamber static pressure was kept below 40 Pa (0.3 mm of mercury). Desired test pressures were generated by the impact pressure of the hypervelocity flowfield and verified by a 10.03 cm o.d. water-cooled pressure model.

Test specimens were subjected to constant surface temperature heating cycles. In these heating cycles, by slightly varying the current to the arc heater, the surface temperature of the test specimens, as recorded by the optical pyrometer, was maintained at a predetermined value.

DTA Tests

DTA tests were conducted at temperatures of 1533–1811 K (2300–2800°F) at stagnation pressures of 0.01, 0.03, 0.05, and 0.07 atm (Table 1). The test conditions provide a wide range of temperature, at limited pressures, with which to evaluate surface sealant loss. Weight loss measurements were used to calculate mass loss rates for the various test conditions. Microscopic analyses were then used to estimate the surface

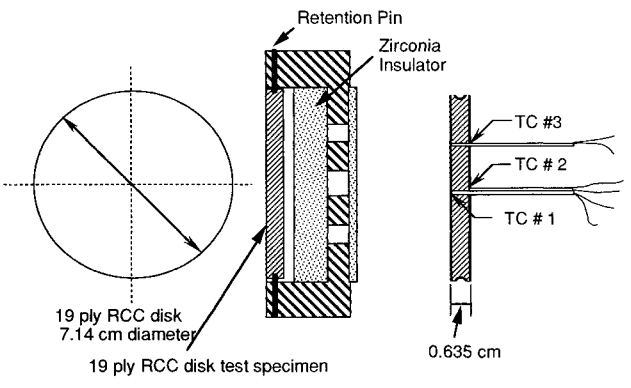

Fig. 1 Test configuration with the RCC test specimen installed in the model holder.

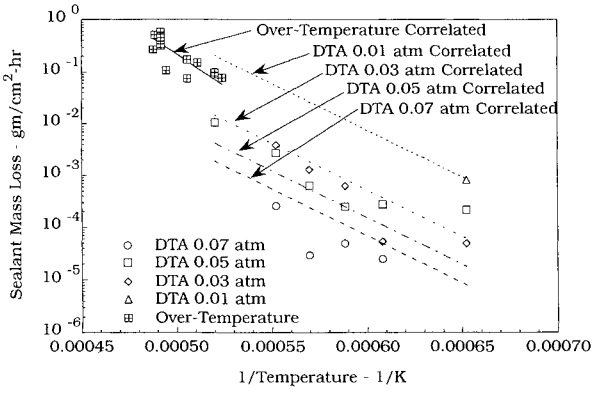

Fig. 2 DTA and over-temperature sealant experimental mass loss rate data compared to correlated mass loss rates.

Table 1 DTA sealant test conditions and mass loss

Stagnation pressure, atm	Pyrometer temperature, K	Specimen	Time, h	Mass loss, gm	Stagnation pressure, atm	Pyrometer temperature, K	Specimen	Time, h	Mass loss, gm
0.07	1811	1B23	8	0.100	0.05	1811	1A23	8	0.568
		2B23	8	0.069			2A23	8	1.211
	1756	1B21	8	0.002		1756	1A21	6	0.132
		2B21	8	0.016			2A21	6	0.185
	1700	1B19	8	0.011		1700	1A19	8	0.085
		2B19	8	0.021			2A19	8	0.082
	1644	1B17	8	0.007		1644	1A17	9	0.088
		2B17	8	0.009			2A17	8	0.103
						1533	1A15	5	−0.008
							2A15	6	0.054
0.03	1811	1B22	5	0.822					
		2B22	5	0.749					
	1756	1A22	5	0.270					
		2B20	5	0.258					
	1700	1B18	8	0.204	0.014	1700	1A18	6	0.803
		2B18	8	0.208			2A18	6	0.695
	1644	1B16	8	0.014		1644	1A16	6	0.385
		2B16	8	0.021			2A16	6	0.411
	1533	1B14	8	−0.011	0.01	1533	1A14	8	0.168
		2B14	8	0.016			2A14	8	0.230

Table 2 Arrhenius equation constants

Description	k, gm/cm²-h	E/R, K	n	Temperature range	
				Low, K	High, K
Sealant					
DTA	7.17822×10^{3}	−41,421.7	−2.4108	1,533	1,922
Over-temperature	1.58949×10^{11}	−54,623.2	0.0	1,908	2,117
SiC					
Diffusion	1.71227×10^{1}	0.0	0.0	2,136	2,478
Rate	1.06363×10^{47}	−225,226.9	0.0	1,967	2,136
Low-temperature cutoff	1.84630×10^{-3}	0.0	0.0	1,811	1,967
Carbon					
Rate	1.57251×10^{3}	−8,085.9	0.5	1,056	1,867
Diffusion	2.02865×10^{1}	0.0	0.5	1,867	2,478

Table 3 Sealant over-temperature test conditions and mass loss

Specimen	Pyrometer temperature, K	Stagnation pressure, atm	Time, s	Mass loss, gm
IN-14	2050	0.146	223	0.660
IN-28	2047	0.147	900	5.091
2	2033	0.049	330	1.643
AB-16	2033	0.049	330	1.244
18	2033	0.083	330	1.737
14	2033	0.083	600	2.093
5	2033	0.151	330	2.108
IN-22	2022	0.143	330	0.392
AB-15	1978	0.043	330	0.628
AC-22	1978	0.047	3300	2.730
4	1956	0.151	330	0.551
3	1922	0.076	330	0.358
16	1922	0.076	800	0.810
AB-13	1908	0.045	353	0.303

sealant and silicon carbide thicknesses. Test specimens were cross sectioned to determine any subsurface oxidation. Photomicrographic examinations of the cross sections of the DTA specimens revealed no substrate oxidation. Therefore, the mass loss rates determined from these tests are considered to be only surface sealant (Na_2SiO_3) loss.

Sealant loss rates, at constant pressures, are shown in Fig. 2 which is typical of an Arrhenius form of mass loss rate with the reciprocal of temperature. A definite dependency of pressure on the sealant loss is exhibited, therefore, the test data was correlated using the following equation:

$$\dot{m} = k(p/p_0)^n e^{-E/RT} \tag{1}$$

where $\dot{m}$ is the mass loss rate per unit area, k is the pre-exponential coefficient in the same units as $\dot{m}$, E/R and T are units of temperature, p is the stagnation pressure, and p_0 is the reference pressure at 1 atm in the same units as p. This

Table 4 SiC over-temperature test conditions and recession depth

Specimen	Pyrometer temperature, K	Stagnation pressure, atm	Sealant start time, s	SiC start time, s	SiC end time, s	Test end time, s	Recession depth, cm
IN-06	2117	0.048	18	42	74	74	0.067
IN-12	2061	0.150	17	114	150	330	0.085
IN-08	2089	0.154	16	79	110	110	0.076
IN-18	2089	0.154	25	72	105	330	0.080
IN-29	2117	0.154	22	102	132	132	0.061
IN-04	2111	0.159	12	44	74	74	0.084
IN-20	2100	0.160	12	43	82	95	0.083
IN-26	2117	0.160	13	19	64	65	0.072
AT-15	2117	0.160	14	53	87	87	0.083
IN-23	2061	0.148	22	70	900	900	0.022
IN-14	2050	0.146	22	77	223	223	0.018
IN-19	2050	0.142	22	77	3,600	3,600	0.047
IN-21	2033	0.138	22	90	1,200	1,200	0.032
IN-25	2033	0.050	22	90	3,600	3,600	0.020
IN-22	2022	0.143	22	102	330	330	0.003
389E04	1811	0.050	20	2,620	28,800	28,800	0.008
TA3-02	1811	0.050	20	2,620	28,800	28,800	0.005

Table 5 RCC carbon substrate over-temperature test conditions and recession depth

Specimen	Temperature, K	Stagnation pressure, atm	Test time, s	Recession depth, cm
28	1056	0.035	4500	0.099
27	1256	0.047	525	0.084
25	1256	0.091	600	0.104
26	1444	0.098	500	0.157
IN-34	1478	0.050	600	0.196
32	1644	0.047	400	0.269
IN-31	1711	0.085	330	0.218
NH-7	1728	0.142	300	0.241
23	1839	0.028	180	0.140
29	1867	0.047	200	0.180
IN-30	2011	0.142	153	0.208
IN-24	2106	0.147	150	0.239
NH-8	2144	0.142	120	0.193

equation can be used for predicting sealant loss over the temperature range of 1533–1811 K; 0.01–0.07 atm (see Table 2).

Over-Temperature Test Results

Over-temperature tests were performed at the conditions shown in Tables 3–5.[6] Negligible surface recession of the RCC SiC coating has been observed at temperatures below 1967 K (3080°F); however, between 1967–2136 K (3080–3385°F) a steady increase in the surface recession is observed. At 2136 K (3385°F), a SiC diffusion limited erosion is observed.

The oxidation mechanisms observed during these high-temperature 1922 K-2117 K (3000–3350°F) tests, follow the classic passive/active oxidation reactions as reported by Schiroky et al.,[9] Rosner and Allendorf,[10] Gulbransen and Jansson,[11] and Strife[12] associated with sodium silicates, glass, and silicon carbide. As a result of the TEOS impregnation and sodium silicate sealant, a protective SiO_2 film protects against active oxidation. As the temperature increases, SiO_2 melts and flows; SiO gas forms at the SiO_2–SiC interface and within the specimen. This activity dramatically increases at approximately 2061 K (3250°F), resulting in an eruption of bubbles on the specimen surface and mechanical disruption of the film. Exposure of the SiC then results in an aggressive active oxidation resulting in a coating breach and exposure of the bare carbon substrate. These complex high-temperature chemistry mechanisms are further complicated by corresponding changes in the material catalytic efficiency and emissivity of the RCC surface and TEOS impregnated substrate.

Sealant loss: weight loss and thickness measurements were used to calculate mass loss/surface recession rates for the various test conditions (Table 3). The DTA tests provided sealant loss data for a temperature range of 1533–1811 K. The over-temperature tests provide sealant loss data from 1867 to 2033 K (2900 to 3200°F). This sealant loss data, shown in Fig. 2, is somewhat higher than the DTA sealant loss data and does not appear to be pressure sensitive. This is a result of more aggressive melting/oxidation reactions on the RCC surface at these higher temperatures. Sealant loss in this temperature range has been correlated using Eq. (1) and the coefficients given in Table 2. Predicted sealant recession depth can be computed using these coefficients and the sealant density of 1.730 gm/cm^3.

Coating recession: silicon carbide recession rate calculations were made using three test parameters: 1) temperature, 2) pressure and time duration, and 3) pre- and post-test coating thickness measurements at several locations on the test specimens (Table 4). Determination of the time duration of the coating breach (SiC loss) was made using the recorded temperature time history. SiC coating recession rate was calculated by dividing the coating loss by time duration. Figure 3 is a plot of the normalized recession rate variation with reciprocal of temperature (i.e., Arrhenius form). As previously discussed, the recession rate is negligible for temperatures less than 1967 K (3080°F) between 1967–2136 K (3080–3385°F), a steady increase in recession rate is observed. At 2136 K (3385°F) a constant recession rate occurs independent of surface temperature, and exhibits a diffusion limited behavior. Coating mass loss has been correlated with Eq. (1) and the coefficients shown in Table 2. Predicted coating recession depth can be computed us-

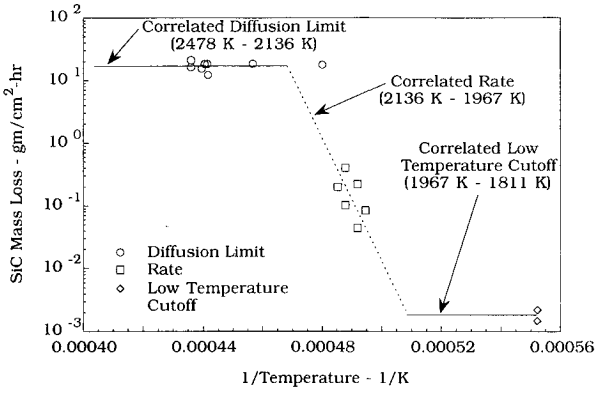

Fig. 3 SiC coating experimental mass loss rate data compared to correlated mass loss rates.

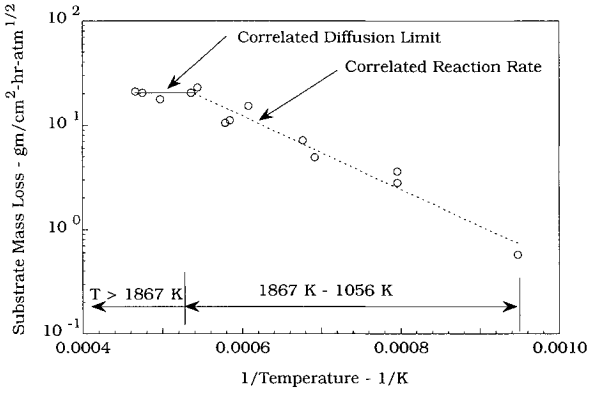

Fig. 4 RCC carbon substrate experimental mass loss rate data compared to correlated mass loss rates.

ing these coefficients and the coating density of 2.114 gm/cm^3.

Substrate recession: an extensive literature database, both analytical and experimental, exists for the oxidation characteristics of bare carbon. Initial oxidation studies by Scala[13] were used to estimate the reaction rate/diffusion limits. Therefore, the objective of this test series was the determination of the RCC substrate recession rate once the SiC coating had been depleted and the substrate was directly exposed to the oxidizing environment.

Specimens were tested over a temperature range of 1033–2144 K (1400–3400°F) (Table 5). Since oxidation of the RCC substrate is initiated at a relatively low temperature, it was important to minimize this oxidation during the initial temperature transient. This was accomplished by using 100% nitrogen test gas during the initial transient period followed by an instantaneous switch to air test gas. Surface recession rate data exhibits a well-defined reaction rate, but the expected diffusion limit at the higher temperature is not as well-defined due to the RCC substrate being impregnated with TEOS (see Fig. 4). This data was correlated with Eq. (1) and the coefficients given in Table 2. Predicted substrate recession depth can be computed using these coefficients and the substrate density of 1.362 gm/cm^3.

Analysis Results

Predictions of sealant loss, silicon carbide, and bare RCC mass loss are compared to plasma Arc test results, thermochemical ablation theory, and for typical Orbiter entries.

Plasma Arc Tests

Equilibrium stagnation heating was calculated using the stagnation enthalpy, pressure, and pressure distribution. Adjustments were made to the stagnation enthalpy to match the measured heating rates. The effective radius was corrected from 5.08 to 16.764 cm using the method described by Hiester and Clark[14] to correct the heating from a hemispherical body to a blunt axisymmetric body. The equation used is given as

$$R_{\text{effective}} = R_{\text{hemisphere}} = 3.3R_{\text{flat face}} \quad (2)$$

A modified version of the boundary-layer integral matrix program (BLIMP)[15] with a built-in radiation equilibrium iteration procedure was used for these calculations. The results of this calculation using the RCC emissivity provided excellent approximations to the reported calorimeter heating.

Since the excellent agreement between the predicted heating for equilibrium flow and the calorimeter data were obtained, the same stagnation conditions were used for heating conditions for nonequilibrium flow. Sambamurthi's upper limit curve fits to the NASA/Ames recombination coefficient data[16] for surface catalysis for reaction-cured glass as reported by Rochelle[17] were used in this calculation. The calculation method used in the present work uses a five-species (N, O, NO, N_2, O_2) air model with equilibrium edge conditions.

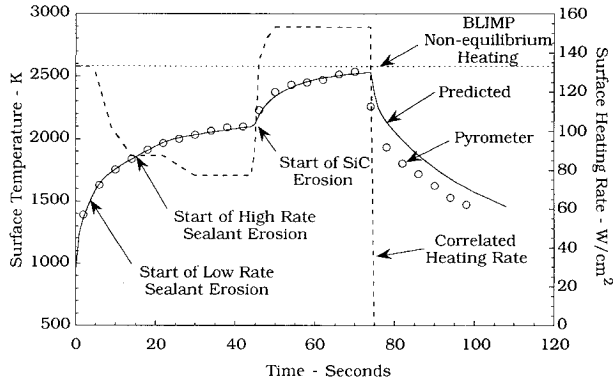

Fig. 5 Comparison between predicted and experimental surface temperatures and heating rates for specimen IN-06.

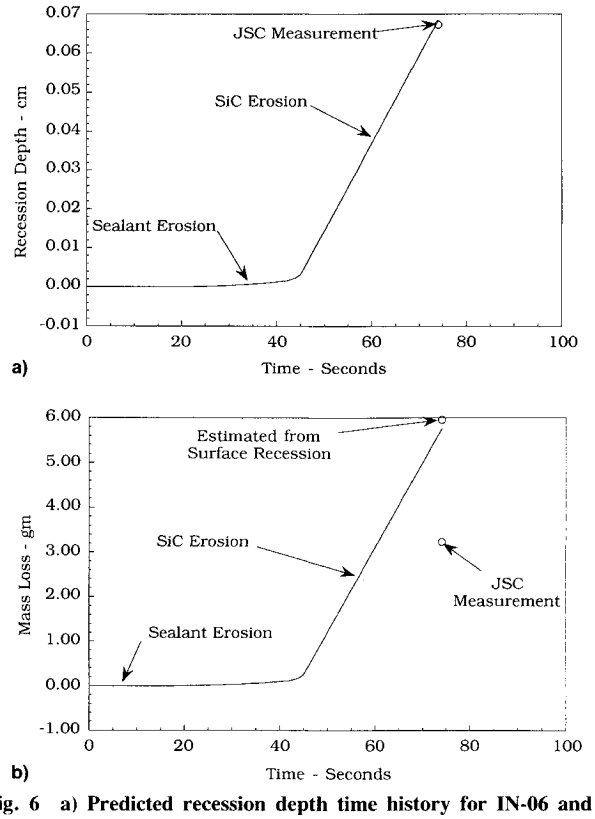

Fig. 6 a) Predicted recession depth time history for IN-06 and b) predicted mass loss history for IN-06.

Two over-temperature test conditions have been selected to compare predicted RCC response with test data: 1) IN-06, 2117 K, 0.048 atm, steady-state test and 2) AU-05, simulated Orbiter abort condition, transient test.

Figure 5 shows the predicted heating and corresponding measured and predicted surface temperature for test IN-06. In this figure abrupt changes in the correlated heating rate indicate the various states of thermochemical activity. Predicted mass loss, shown in Fig. 6, consists of sealant loss followed by silicon carbide erosion. The endothermic and exothermic behavior of sealant and SiC erosion processes are obvious. The correlated heating rate during sealant loss is approximately 60% of the BLIMP heating for nonequilibrium flow; while during silicon carbide erosion, the correlated heating is approximately 18% higher than the BLIMP heating for nonequilibrium flow. These heating variations are attributed to surface chemical reactions, wall emissivity, and surface catalytic effects. Predicted mass loss is compared to the test data using two approaches; coating thickness and weight loss measurements. Measured mass loss using coating thickness compares well with prediction (Fig. 6a); mass loss using weight change results shows a conservative/overprediction of the mass loss (Fig. 6b). This is not unexpected since the maximum coating thickness erosion was used in the calculation of measured mass loss and the weight change is an average over the entire specimen.

Figure 7 shows the predicted heating and corresponding measured and predicted surface temperature for test AU-05, which simulated a typical abort condition. Predicted recession depths and mass loss, shown in Fig. 10, consist of sealant and SiC loss. Once again during sealant loss, the convective heating is less (≈60%) than the BLIMP nonequilibrium value. The heating variations are attributed to surface chemical reactions, wall emissivity, and surface catalysis. The recession depth (Fig. 8a) is within 33, 23, and −2.3% of the thickness change measurements reported by JSC, Loral, and Rockwell, respectively.[6,18] The predicted mass loss is conservatively estimated when compared with measured mass loss (Fig. 8b) by over 160%.

Thermochemical Ablation Theory

Thermochemical ablation for the oxidation protected RCC is compared with data obtained from the JSC Arc-Jet plasma tunnel. The computer code utilized herein is the Aerotherm Chemical Equilibrium (ACE) program.[19] This program solves for surface elemental mass balances, producing solutions for ablation rate normalized by mass-transfer coefficient in terms of pressure, surface temperature, and normalized pyrolysis gas rate. A variety of physicochemical models can be assumed including consideration of equilibrium or rate-controlled reactions at the surface and mechanical removal of candidate surface species.

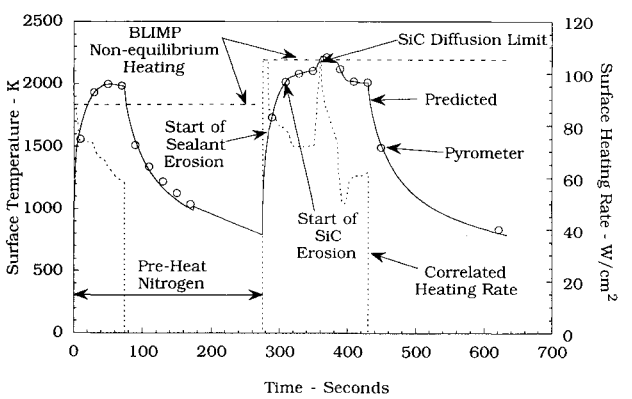

Fig. 7 Comparison between predicted and experimental surface temperatures and heating rates for abort simulation (AU-05).

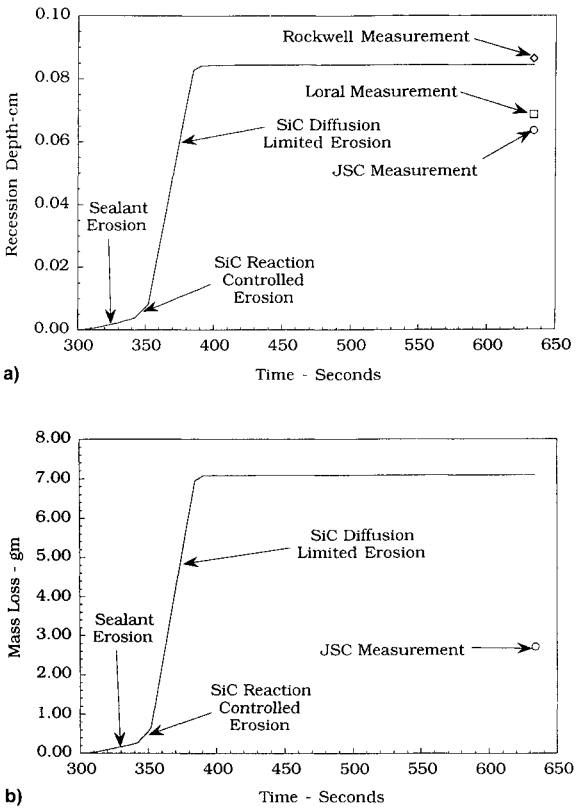

Fig. 8 a) Predicted recession depth history for the abort simulation (specimen AU-05) and b) predicted mass loss history for the abort simulation (specimen AU-05).

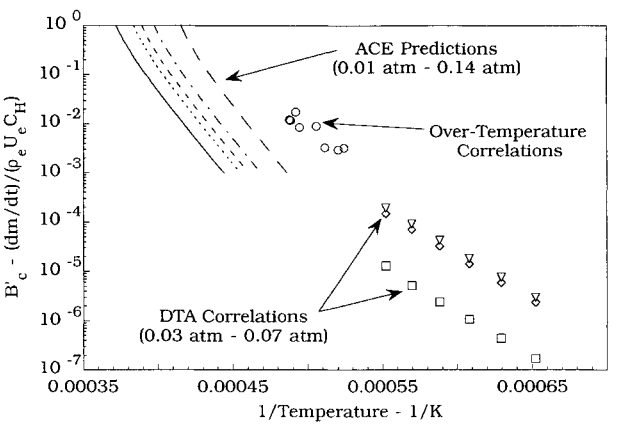

Fig. 9 Comparison of Na_2SiO_3 ablation rates calculated by ACE and sealant correlations using Arc-Jet test data.

An open system analysis was performed for a sodium silicate system with 30 species at conditions corresponding to the DTA test pressures. The species selected were based on Na, Si, C, O, and N atoms. The boundary layer consists of 78% N and 22% O (with a small fraction of C) with two parts sodium and one part Si for three parts O (Na_2SiO_3) for the char material. The pyrolysis gas rate was set to zero, since sodium silicate does not decompose in depth, but either melts or vaporizes. Nondimensional char rates

$$B'_c = \dot{m}/(\rho_e u_e C_H) \tag{3}$$

were varied from 1 to 10^{-7} for this analysis. (The subscripts c and e refer to char and edge conditions, respectively. C_H is the heat transfer coefficient, whereas m, ρ, and u refer to the mass, density, and velocity, respectively.) The results presented in Fig. 9 indicate that the assumptions for chemical

Table 6 RCC sealant mass loss predictions for atmospheric re-entry flight environments on the wing leading edge (panel 9)

Type of flight trajectory	Sealant loss per flight, cm/flight	Sealant mission life, no. of flights: Sealant thickness, 0.00254 cm	Sealant thickness, 0.00381 cm	Sealant thickness, 0.00508 cm
Nominal, STS-30	0.000404139	6	9	12
Heavyweight	0.000561517	4	6	9
Transoceanic abort landing	0.003561080	Less than one	1	1

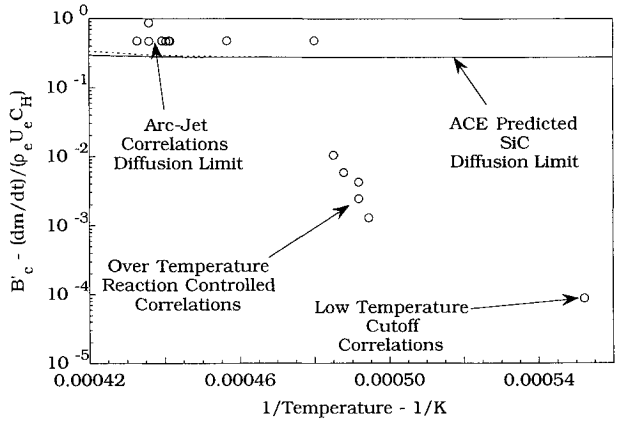

Fig. 10 Comparison of SiC ablation rates calculated by ACE and SiC coating correlations using Arc-Jet test data.

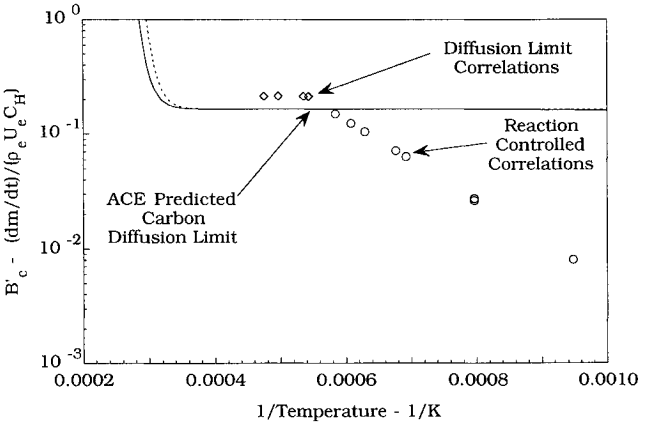

Fig. 11 Comparison of carbon ablation rates calculated by ACE and carbon substrate correlations using Arc-Jet test data.

equilibrium below 2500 K are not accurate. Data from the DTA and over-temperature tests[6] are shown in Fig. 9 compared to the ACE-predicted data, but the predictions are in poor agreement for low temperature (1500–2033 K) convective ablation data. This is attributed to ACE being limited to a single condensed species and nonconvergent solutions.

These results were as expected since there is no chemical means for removing Na_2SiO_3 from the surface until the temperature is sufficiently high that decomposition takes place. There are reasons that one might expect at least some mechanical removal of the sealant at surface temperatures below 2500 K. First, the sodium silicate melts at lower temperatures, and there will be some removal by liquid-layer flow. The loss of sealant in this manner was observed in the videos of tests, and liquid globules were found on the surface after cooldown. The use of an artificial fail temperature for Na_2SiO_3 in ACE would be required to predict sealant loss in the low temperature regime; therefore, Arrhenius equations were developed

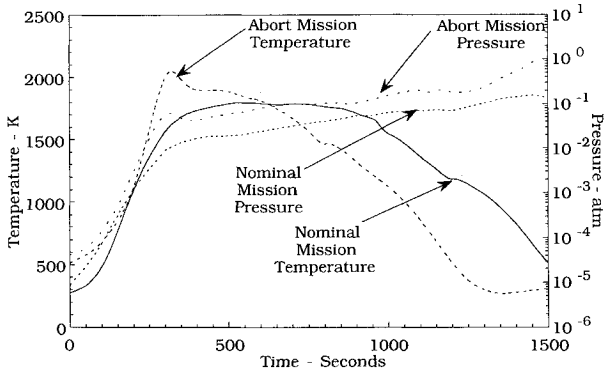

Fig. 12 Stagnation point surface temperature and pressure on the wing leading edge panel 9 for nominal and abort missions.

to predict sealant erosion for the surface temperature range 1500–2033 K.

In a similar manner, ACE predictions were made for a silicon carbide surface. Figure 10 compares the test data with ACE predictions. Once again, the dominant effect of the SiO, SiO_2, and Si species on the SiC mass loss rate is apparent. Only at the higher temperature (≈2060 K) do the ACE predictions agree with the test data; where the test data indicate a SiC diffusion limit.

The third stage of the oxidation protection RCC material ablation is bare carbon–carbon recession. ACE predictions for pure carbon are compared with bare RCC recession in Fig. 11. The incorporation of TEOS into the RCC substrate inhibits the carbon oxidation at the lower temperatures, but reasonable agreement with ACE and diffusion limit theory is obtained at the higher temperatures.

Flight Predictions

The single mission limit and/or reusability of the RCC components can now be predicted using sealant, coating, and bare carbon–carbon correlations. Mission life predictions require an additional equation to predict subsurface oxidation.[7] Therefore, we will restrict these predictions to sealant loss and SiC erosion. Routine Shuttle Orbiter entries have little or no surface recession. However, extension of the Orbiter flight envelope certification to high inclination, heavyweight, and abort entries results in high surface temperatures (>1867 K). Typical temperature/pressure profiles for a nominal and abort entry are shown in Fig. 12. The higher surface temperature associated with the abort entry results in a greater sealant loss. Predicted sealant loss for nominal, heavyweight, and abort entry is shown in Table 6. Using these calculations, it takes approximately 9 heavyweight and 12 nominal entries to remove a 2-mil surface sealant thickness. Postflight inspection of the Orbiter Columbia indicates local loss of surface sealant after 12 flights, which is consistent with the predictions. However, minimal surface recession is predicted using the correlations, which is consistent with a passive state of SiC oxidation during entry.[20] Although surface sealant is ablated for abort entries, very little surface recession occurs as seen

in Table 6. These results show that a single engine out abort can be safely flown, but RCC refurbishing would be required prior to the next flight.

Error Analysis

A detailed discussion on the accuracy of the correlation coefficients tabulated in Table 2 can be found in the error analysis by Williams et al.[21] A summary of these results is presented in the following text.

Calibration models were used to correlate surface temperatures measured with thermocouples with the laser pyrometer. The recorded laser pyrometer surface temperature was within 5% of the measured thermocouple surface temperature. The laser pyrometer starts recording temperatures when the surface reaches approximately 810 K.

Sealant loss: the sealant mass loss predictions are shown in Fig. 2. The DTA error assessments for each pressure are: $+0\%/-75\%$ @ 0.07 atm, $+150\%/-0\%$ @ 0.05 atm, $+0\%/-40\%$ @ 0.03 atm, and $+30\%/-40\%$ @ 0.01 atm. The large difference for the 0.05-atm data is not surprising since the 0.03-atm data and 0.05-atm data are almost indistinguishable.

Coating recession: the SiC coating mass loss predictions are shown in Fig. 3. The diffusion limit error bands were computed to be $\pm 10\%$. The low-temperature cutoff error bands were computed to be $\pm 20\%$. There was more scatter for the rate-controlled recession with the error bands assessed to be $+90\%/-50\%$. Although it appears as if more accuracy is given to the low-rate data than to the high-rate data, the regression line in Fig. 3 appears to evenly divide the data.

Substrate recession: the RCC substrate mass loss predictions are shown in Fig. 4. The diffusion limit error bands were computed to be $\pm 10\%$, and the error bands for the rate-controlled recession were computed to be $\pm 20\%$.

The error analysis indicates that the correlations can be used with confidence to predict sealant loss, coating recession, and substrate mass loss for flight conditions.

Summary

The RCC material has demonstrated outstanding high-temperature thermal structural characteristics during its application to the leading-edge structural system for the Space Shuttle Orbiter. Oxidation performance testing of the RCC in plasma arc heating facilities was conducted to develop surface sealant (Type A) mass loss correlations. Over-temperature testing was performed to establish coating (silicon carbide) recession for temperatures in excess of the multimission temperature limit. The resulting database and correlations have been successfully applied in extending the Orbiter flight envelope and ensuring safety of flight for off-nominal (abort) entries.

Based on the ground test results, correlations/analyses, and flight performance, the Orbiter RCC system is expected to achieve its full mission life objectives and retain an over-temperature capability for potential mission abort conditions.

Acknowledgments

The authors of this article acknowledge the following people for their significant efforts in the RCC Testing and Analyses: Ignacio Norman, Jesus Reyna Jr., and Scott Christensen of Rockwell International Corporation; Neal Webster of Loral Vought Systems; and Jim Milhoan and Don Tillian of the NASA Johnson Space Flight Center.

References

[1]Medford, J. E., "Prediction of Oxidation Performance of Reinforced Carbon-Carbon Material for Space Shuttle Leading Edges," AIAA Paper 75-730, May 1975.

[2]Medford, J. E., "Prediction of In-Depth Oxidation Distribution of Reinforced Carbon-Carbon Material for Space Shuttle Leading Edges," AIAA Paper 77-783, June 1977.

[3]McGinnis, F. K., "Shuttle LESS Subsurface Attack Investigation Final Report," Vought Corp., Rept. 221RP00241, Dallas, TX, 1974.

[4]Webster, C. N., "March 1984 Radiant Mass Loss Correlation—RCC/Coated/TEOS/Type A," Vought Corp., Dir 3-53200/RCC/4-003, Dallas, TX, March 1984.

[5]Webster, C. N., "June 1984 Convective Mass Loss Correlation—RCC/Coated/TEOS/Type A," Vought Corp., Dir 3-53200/RCC/4-006, Dallas, TX, June 1984.

[6]Milhoan, J. D., Pham, V. T., and Yuen, E. H., "Compilation of Reinforced Carbon-Carbon Transatlantic Abort Landing Arc Jet Test Results," NASA TM 104778, Dec. 1993.

[7]Curry, D. M., Yuen, E. H., Chao, D. C., and Webster, C. N., "Space Shuttle Orbiter Carbon-Carbon Oxidation Performance," *Damage and Oxidation Protection in High Temperature Composites-Vol. 1*, AD-Vol. 25-1, American Society of Mechanical Engineers, 1991, pp. 47–64.

[8]Rochelle, W. C., Battley, H. H., Tillian, D. J., Grimaud, J. E., Murray, L. P., Lueke, W. J., and Heaton, T. M., "Orbiter TPS Development and Certification Testing at the NASA/JSC 10 MW Atmospheric Reentry Materials and Structures Evaluation Facility," AIAA Paper 83-0147, Jan. 1983.

[9]Schiroky, G. H., Price, R. J., and Sheehan, J. E., "Oxidation Characteristics of CVD Silicon Carbide and Silicon Nitride," GA Technologies, Rept. GA-A18696, San Diego, CA, 1986.

[10]Rosner D. E., and Allendorf, H. D., "High Temperature Kinetics of the Oxidation and Nitridation of Pyrolytic Silicon Carbide in Dissociated Gases," *Journal of Physical Chemistry*, Vol. 74, No. 9, 1970, pp. 1829–1838.

[11]Gulbransen, E. A., and Jansson, S. A., "The High-Temperature Oxidation, Reduction and Volatilization Reactions of Silicon and Silicon Carbide," *Oxidation of Metals*, Vol. 4, No. 3, 1972, pp. 181–201.

[12]Strife, J. R., "Development of High Temperature Oxidation Protection for Carbon-Carbon Composites," United Technologies Research Center, Rept. NADC-91013-60, March 1990.

[13]Scala, S. M., and Gilbert, L. M., "Sublimation of Graphite at Hypersonic Speeds," *AIAA Journal*, Vol. 3, No. 9, 1965, pp. 1635–1644.

[14]Hiester, N. K., and Clark, C. F., "Feasibility of Standard Evaluation Procedures for Ablating Materials," NASA CR-379, Feb. 1966.

[15]Murray, A. L., "Further Enhancements of the BLIMP Computer Code and User's Guide," Air Force Wright Aeronautical Labs., AFWAL-TR-88-3010, June 30, 1988.

[16]Kolodziej, P., and Stewart, D. A., "Nitrogen Recombination on High Temperature Reusable Surface Insulation and the Analysis of Its Effect on Surface Catalysis," AIAA Paper 87-1637, June 1987.

[17]Rochelle, W. C., and An, M. Y., "Leading Edge Structural Subsystem (LESS) Entry Heating Study—Final Report, Volume I—Methodology and Results," Lockheed Engineering and Sciences Co., LESC-30453, Houston, TX, May 1993.

[18]Webster, C. N., "RCC Recession Rates from Overtemperature Test Data," Vought Corp., Dir 3-56700/RCC/1-0001, Dallas, TX, May 1991.

[19]Anonymous, "User's Manual Aerotherm Chemical Equilibrium Computer Program (ACE 81)," Acurex Corp., UM-81-11/ATD, Mountain View, CA, Aug. 1981.

[20]Williams, S. D., Curry, D. M., Chao, D. C., and Vuong, P. T., "Ablation Analysis of the Shuttle Orbiter Oxidation Protected Reinforced Carbon-Carbon," AIAA Paper 94-2084, June 1994.

[21]Williams, S. D., Curry, D. M., Chao, D. C., and Vuong, P. T., "Ablation Analysis of the Shuttle Orbiter Oxidation Protected Reinforced Carbon-Carbon," NASA TM 104792, June 1994.